*Armenian Journal of Physics, 2024, vol. 17, issue 3, pp. 43-51*

# Numerical Solutions of Certain Time-Independent Quantum Mechanics Problems by Using the Python Environment

H. Shahinyan, L. Ghazaryan, A. Babajanyan

*Institute of Physics, Yerevan State University, A. Manoogian 1, 0025 Yerevan, Armenia*

E-mail: barsen@ysu.am

(Received: June 21, 2024; Revised: November 10, 2024; Accepted: November 17, 2024)

**Abstract.** This paper discussed the digitization of some analytical solutions of the fundamental equation of non-relativistic quantum mechanics, the Schrödinger equation, in the Python programming environment. The main objective of the work is to automate the solution of several known analytically solvable problems of quantum mechanics and ensure their use in more complex problems. For this purpose, the Python programming environment was chosen, which, due to the large number of libraries and flexibility, is currently widely used in solving physical and mathematical problems. In the program we propose, which is available on the GitHub platform, it is solved easily. The problem of determining the probability of the spatial distribution of an electron in a hydrogen-like atom is discussed. The Schrödinger equation is presented in the spherical coordinate system. The wave function, describing the electron's state, quantized energy values, and probability density, is derived analytically. A recursive function was written in Python to handle the series coefficients defining the wave function. Utilizing relevant libraries, the resulting program constructs electron spatial distribution functions for different excitation levels. The paper then examines two one-dimensional tunneling scenarios and provides the tunneling coefficients in analytical form. A Python program was developed to plot the dependence of these coefficients on the particle's coordinate and energy. All the code is available on GitHub.

**Keywords:** hydrogen atom, helium ion, spatial distribution, tunneling effect

**DOI: 10.54503/18291171-2024.17.3-43**

## 1. Introduction

We can discuss conserved energy when the quantum system is in a time-independent force field. In quantum mechanics, energy takes on discrete values and is determined from the differential equation of eigenvalues and Eigen functions. That equation was named Schrödinger's equation. It contains the Hamiltonian operator on the left-hand side, defined by either the momentum or coordinate operators in the case of the coordinate and momentum representations, respectively. In the time-independent case, this equation is more straightforward for non-rotating systems. This means that if we do not consider the dependence of the wave function on ϑ and φ, then for the states we are discussing, the angular momentum is also zero, and therefore $l = 0$. Thus, states were studied where the orbital quantum number is zero: $l = 0, n = 1, 2, \ldots$. The radial part of the Schrödinger equation, where the potential energy contains the term $\frac{\hbar^2 l(l+1)}{2mr^2}$, due to the angular momentum [1, 2]. The case $l = 0$ is used to generalize the case $l \neq 0$. The Schrödinger equation [3, 4], a cornerstone of quantum physics, allows for determining the wave function that describes a quantum system's state, thereby enabling the calculation of probability density. As a second-order inhomogeneous linear differential equation with partial derivatives, it can be challenging to solve analytically [5]. The nonlinear form of the Schrödinger equation is discussed in Ref. 6. The first integral of the Hamilton operator is the Laplace operator. Depending on the symmetry of the problem, it can be presented in a Cartesian, cylindrical, or spherical coordinate system. In the first question presented in the paper, the Laplace operator is brought into the spherical coordinate system because the hydrogen atom has spherical symmetry. The results of this problem can be applied to the study of heavier atoms and molecules, especially when describing their "inner" electron states.

In the second question, one-dimensional potential barriers are discussed, and bringing the Laplace operator into the Cartesian coordinate system is advisable. Tunneling problems are essential in researching conductors, semiconductors, and alpha decay properties. Tunneling is also significant in the study of the behavior of elementary particles when the latter is located in the superdense matter in stars [7]. Numerical solutions in the Python programming environment are given to generalize the solutions to the problems discussed. The Python environment was chosen because it is widely used to solve physical and mathematical problems [8]. It can help solve quantum mechanical issues such as the two-particle problem, the problem of solving the Schrödinger equation for molecules (adiabatic approximation), etc.

## 2. Problem 1: Statement and analytical solution

The form of the Laplace operator depends on the specific problem at hand. For problems exhibiting spherical symmetry, the spherical coordinate system is particularly convenient. Hydrogen-like atoms are examples of such systems, where the electron exists within the electrostatic field of a nucleus with charge $q_N = Ze$: $U(r) = -\frac{Ze^2}{r}$, where $r$ is the radius-vector of the electron. If the electron's energy is less than zero, $E < 0$, it is localized in the potential hole $U(r)$. The electron's motion is finite, and its energy is quantized, as determined by solving the fundamental equation of quantum mechanics. The Laplace operator, which is part of the Schrödinger equation, appears as follows in the Cartesian coordinate system: $\Delta = \frac{\partial^2}{\partial x^2} + \frac{\partial^2}{\partial y^2} + \frac{\partial^2}{\partial z^2}$. Given the spherical symmetry of the problem, it is convenient to express the Laplace operator in spherical coordinates. The relationship between spherical and Cartesian coordinates is as follows: $x = rsin\theta cos\varphi,\ y = rsin\theta sin\varphi,\ z = rcos\theta$. In the case under discussion, rotations and time dependence are not considered. The wave function is independent of the rotation angles $\theta$ and $\varphi$, as well as time, and is determined solely by the radial vector $\psi(r)$. The Laplace operator has the following form: $\Delta = \frac{\partial^2}{\partial r^2} + \frac{2}{r}\frac{\partial}{\partial r}$. Calculations have been performed in parabolic coordinates [9] and on an elliptical basis [10].

By applying conditions from Eq.(2) to Schrödinger's stationary Eq.(1) and considering that $E < 0$, which implies $k^2 > 0$, Eq.(3) will be obtained.

$$\frac{d^2\psi}{dr^2} + \frac{2}{r}\frac{d\psi}{dr} + \frac{2m}{\hbar^2}\left(E + \frac{Ze^2}{r}\right)\psi = 0, \tag{1}$$

$$\sigma = \frac{2mZe^2}{\hbar^2}, k^2 = -\frac{2mE}{\hbar^2}, \tag{2}$$

$$\frac{d^2\psi}{dr^2} + \frac{2}{r}\frac{d\psi}{dr} + \frac{\sigma}{r}\psi = k^2\psi. \tag{3}$$

By making the substitution $F(r) = r\psi(r)$ and considering the identity $\Delta\psi(r) = \frac{d^2\psi}{dr^2} + \frac{2}{r}\frac{d\psi}{dr} \equiv \frac{1}{r}\frac{d^2(r\psi)}{dr^2} = \frac{1}{r}\frac{d^2F}{dr^2}$, Eq.(3) will take the following form:

$$\frac{d^2F}{dr^2} + \frac{\sigma}{r}F = k^2F. \tag{4}$$

As $r \to \infty$, the second term on the left side of Eq.(4) becomes smaller than the first term, allowing it to be written as follows:

$$\frac{d^2F}{dr^2} = k^2F. \tag{5}$$

The solution to Eq.(5) takes the form $F \sim e^{\pm kr}$. $F \sim e^{kr}$ diverges as the radius increases, which does not satisfy the wave function's standard conditions. It is more convenient to seek the solution with $F = e^{-kr}f(r)$. In this case, the wave function can be represented as:

$$\psi(r) = \frac{1}{r}e^{-kr}f(r). \tag{6}$$

By substituting $F(r)$ into Eq.(4) and performing mathematical transformations, we derive the differential Eq.(7) for the function $f(r)$, whose solutions take the form of power series as presented in Eq.(8).

$$\frac{d^2f}{dr^2} - 2k\frac{df}{dr} + \frac{\sigma}{r}f = 0, \tag{7}$$

$$f(r) = \sum_0^\infty A_s r^s. \tag{8}$$

Upon inserting Eq.(8) into Eq.(7), we derive the equation $\sum_{s=0}^{\infty}[A_{s+1}s(s+1) - 2ksA_s + \sigma A_s]r^{s-1} = 0$, which must hold for all $r$ values. This implies that all coefficients preceding $r^{s-1}$ are zero. Specifically, when $s = 0$, it follows that $A_0 = 0$. For other values of $s$, a recursive formula in Eq.(9) is obtained, linking successive coefficients in the series from Eq.(8).

$$A_{s+1} = \frac{2ks-\sigma}{s(s+1)}A_s, \ s = 1,2,3, \ldots \tag{9}$$

The wave function $\psi(r)$ remains finite when the coefficients of the series from Eq.(8) start becoming zero from a specific point: $s > n, A_{n+1} = 0$, which brings to the following equation: $2kn - \sigma = 0$. Taking into account Eq.(2), this condition determines the energy value at the $n$–th level as:

$$E_n = -\frac{me^4}{2\hbar^2}\cdot\frac{Z^2}{n^2}, \text{ where } n = 1,2,3, \ldots \tag{10}$$

It is important to highlight that Eq.(10) yields the same result as that for the hydrogen atom with atomic number $Z = 1$, derived within Bohr's semi-classical theory. Hence, the energy levels are quantized according to Eq.(10), and the electron wave function can be expressed as follows:

$$\psi_n(r) = \frac{1}{r}e^{-k_n r}Q_n(r),$$

$$Q_n(r) = A_1 r + A_2 r^2 + A_3 r^3 + \cdots + A_n r^n = \sum_{s=1}^{n} A_s r^s,$$

$$A_{s+1} = \frac{2k_n s-\sigma}{s(s+1)}A_s,$$

$$\sigma = \frac{2me^2}{\hbar^2} = \frac{2}{a}, k_n = \sqrt{-\frac{2mE_n}{\hbar^2}} = \frac{1}{an}. \tag{11}$$

## 3. Problem 1: Results and discussion

In the specific scenario when $n = 1$, the wave function for the ground state is defined as: $\psi_1(r) = A_1 e^{-k_1 r}$, and $k_1 = \frac{Zme^2}{\hbar^2} = \frac{Z}{a}$. The coefficient $A_1$ is determined by the normalization condition of the wave function: $\int |\psi|^2 dV = \int_0^\infty A_1^2 e^{-2k_1 r} 4\pi r^2 dr = 1$, from which we get $A_1 = \sqrt{\frac{k_1^3}{\pi}} = \sqrt{\frac{Z^3}{\pi a^3}}$. Therefore, the wave function for in the ground state of the hydrogen atom with $Z = 1$ is determined by the following formula: $\psi_1(r) = \sqrt{\frac{1}{\pi a^3}} e^{-k_1 r}$, where $k_1 = \frac{1}{a}$.

The probability of the electron's spatial distribution is determined by $|\psi_1(r)|^2 dV$ [11, 12], representing the probability of detecting an electron within the volume $dV$. Utilizing the spherical coordinate system, this probability within a spherical shell of radius $r$ and thickness $dr$ is given by [13]

$$dW_1(r) = w_1(r)dr = \frac{1}{\pi a^3} e^{-2r/a} 4\pi r^2 dr. \qquad (12)$$

It is a known fact that an exponential function decreases faster than a power function can increase. This indicates that the probability density $w_1(r) = dW_1/dr$ achieves its maximum value at a certain $r$. The value of $r$ corresponding to that maximum density can be determined from the following equation: $\frac{dw_1(r)}{dr} = 0$. Using Eq. (12), the following quantity is obtained: $r_{max} = a = \frac{\hbar^2}{me^2}$. $r_{max}$ is the distance from the nucleus in a hydrogen atom where the probability of finding an electron is highest. For hydrogen-like atoms, the value of $r_{max}$, given $Z$, is determined by the formula: $r_{max} = a = \frac{\hbar^2}{mZe^2}$. Here are the numerical evaluations: $a = 0.529\, A^0 = 0.529 \cdot 10^{-8}\, cm$. This implies that the dimensions of the hydrogen atom are $d = 2a \approx 1\, A^0$, which aligns with experimentally obtained dimensions.

For the second excited level, $\psi_2(r) = (A_1 + A_2 r)e^{-k_2 r}$ is derived, where $A_2$ is obtained from the recursive Eq. (11): $\psi_2(r) = A_1 \left(1 - \frac{r}{2a}\right) e^{\left(-\frac{r}{2a}\right)}$, and the coefficient $A_1$ is determined by the normalization condition: $\int |\psi_2|^2 dV = \int_0^\infty |\psi_2|^2\, 4\pi r^2 dr = 1$, $A_1 = \frac{1}{\sqrt{8\pi a^3}}$. It's noteworthy that the wave function $\psi_2(r)$ has a zero value at a distance equal to twice the Bohr radius, specifically when $r = 1/k_2 = 2a$. The probability of detecting an electron at a distance $r$ from the nucleus is determined by the following formula: $dW_2(r) = w_2(r)dr = {A_1}^2 (1 - \frac{r}{2a})^2 e^{-r/a} 4\pi r^2 dr$.

The function $w_2(r)$ exhibits four extrema: two maximums and two minimums. The first minimum, observed in both $n = 1$ and the current case, coincides with the center of the atom, $r = 0$. The second minimum occurs at a distance equal to twice the Bohr radius, $r = 2a$, where the wave function $\psi(r)$ for the first excited state becomes zero. The maximum values of the probability density occur at the following distances $r$: $r_1 = \left(3 \mp \sqrt{5}\right)a$.

In the ground state ($n = 1$), the wave function $\psi_1(r)$ has no node within the interval $0 < r < \infty$. In contrast, the first excited state ($n = 2$) wave function $\psi_2(r)$ has one node. As the value of the quantum number $n$ increases, the number of nodes increases. There will be $n - 1$ nodes in the $n$–th state. States with higher quantum numbers, corresponding to higher energies, involve more intricate electron spatial distribution probability functions. This study aims to numerically compute and visually represent these functions, complementing the analytical expressions for spatial distribution probability across any excited state and for any value of $Z$. It's worth noting that obtaining these functions analytically for large quantum numbers is quite challenging. Calculating the coefficients $A_{s+1}$ for each subsequent term in the polynomial $Q_n(r)$, as determined by Eq.(11) using the recursive approach, becomes complex. Therefore, digital methods are employed to solve this problem efficiently.

A program was created in Python that defines a recursive function to determine the coefficients of the polynomial $Q_n(r) = A_1 r + A_2 r^2 + A_3 r^3 + \cdots + A_n r^n$ $(A_{s+1}, s = [1, n])$. Next, the polynomial $Q_n(r)$ and the wave function $\psi_n$ were constructed. Using the definition of probability, the function $w_n(r) = |\psi_n(r)|^2$ was determined for each $n$. Different intervals of the distance from the nucleus, $10^{-20} < r < N * a$, were selected for various ground and excited states. The center of the atom corresponds to $r = 0$, where the program encounters a division by zero error. Therefore, the starting point for the calculations was set to $10^{-20}$. The spatial distribution probabilities $w_1(r)$, $w_2(r)$, and $w_3(r)$ were plotted using the *Matplotlib.pyplot* library in Python for 100 points within the specified ranges of distances from the nucleus. The *Python Numpy* library was utilized to store the data. The Python code is available on GitHub [14].

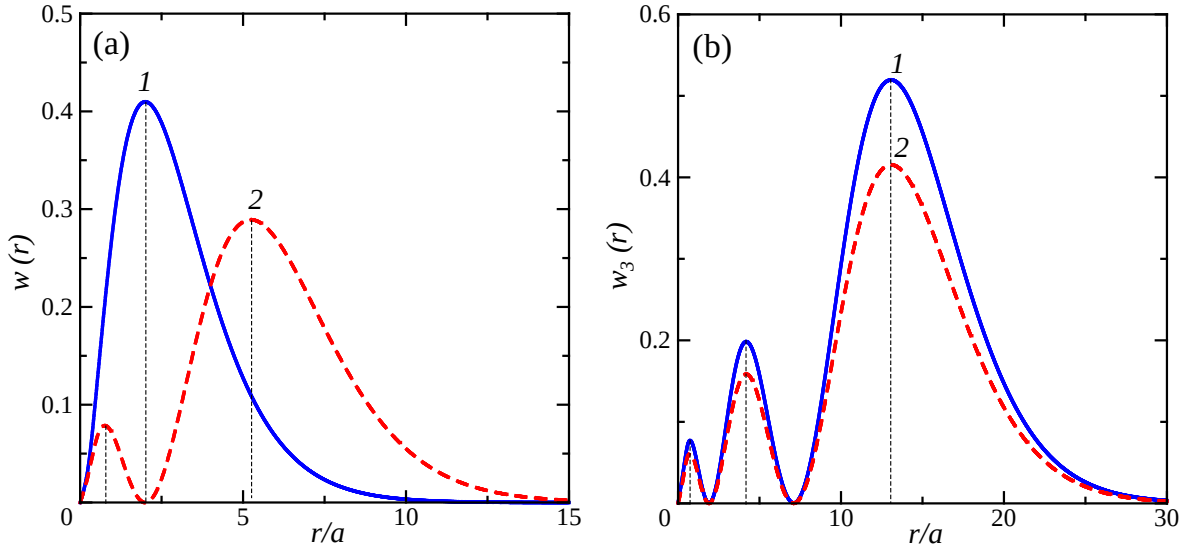


**Fig. 1**. (a) The probability distribution function of finding an electron in a hydrogen atom in the ground state ($n = 1$; curve 1) and the first excited state ($n = 2$; curve 2). (b) Spatial probability distribution for an electron in a hydrogen atom (curve 1) and a helium ion (curve 2) in the second excited state $n = 3$.

Fig.1(a) blue line (curve 1) represents the probability of the electron's spatial distribution in the hydrogen atom's ground state ($n = 1$). The figure shows that the probability peaks at $r = a$, corresponding to the Bohr radius. This indicates that the Bohr radius is significant as it represents the distance from the nucleus where the electron is most likely to be found in the ground state. The probability density decreases exponentially for distances beyond this point, making detecting the electron at greater ranges unlikely. The red line (curve 2) illustrates the spatial distribution probability of the electron in the hydrogen atom's first excited state ($n = 2$). The dotted lines indicate the distances from the nucleus in the hydrogen atom where the probability of finding the electron is highest. The figure shows that there are $n - 1$ nodes for each state where the probability of detecting the electron is zero, corresponding to the quantum number $n$. The spatial distribution probability of an electron in a hydrogen-like atom ($Z \neq 1$) was also determined.

Fig.1(b) shows the spatial distribution probabilities of the electron in the second excited state ($n = 3$) for the hydrogen atom (blue line) and the ionized helium atom $Z = 2$, $He^+$ (red line). As the atomic number $Z$ increases, the probability of the electron distribution at the given excitation level decreases. This occurs because the coefficients determining the wave function decrease with the increasing value of $\sigma$, which, according to Eq.(2), is directly proportional to $Z$. Consequently, as $Z$ increases, the spatial distribution probability of the electron diminishes.

## 4. Problem 2: Statement and analytical solution

Quantum tunneling, a non-equilibrium process, is one of the most fascinating topics in quantum physics. It has been studied in various microscopic systems, including alpha decay of the nucleus [15], quantum cosmology [16], and tunneling in Josephson junctions [17]. The experimental observation of macroscopic quantum tunneling of a Bose-Einstein condensate in a hybrid trap is discussed in [18]. Due to the tunneling, it is possible to explain the theory of the early formation of the Universe [19]. In Ref. 7, it is experimentally shown that solid $H_2O$ is formed by surface $OH + H_2$ reaction, which is possible due to tunnel transitions.

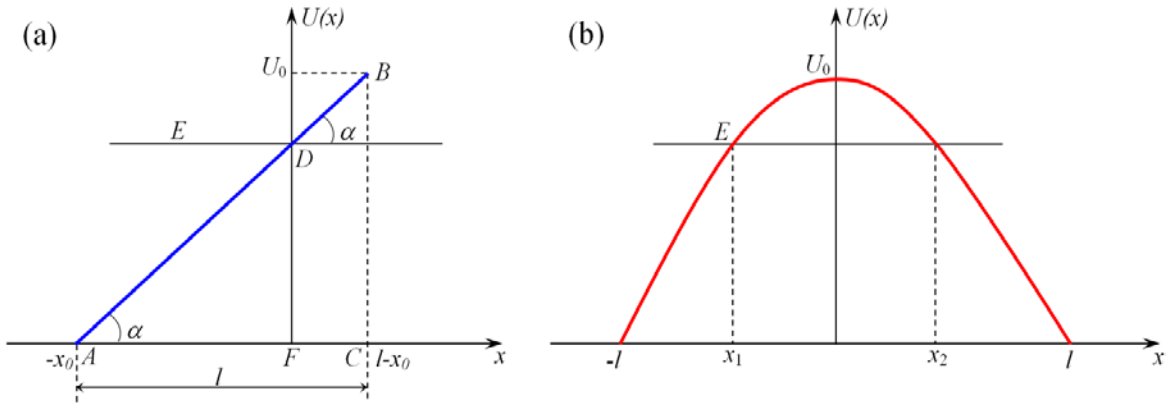


**Fig. 2**. Passage of a quantum particle through a one-dimensional potential barrier: (a) triangular and (b) parabolic, each of length $l$. The barriers reach a maximum height of $U_0$, and the particle with energy $E$ travels in the $x > 0$ direction.

The traversal of a quantum particle with specific energy through one-dimensional potential barriers (tunneling) is explored through solutions to the stationary Schrödinger equation in Cartesian coordinates. This approach represented a direct pathway toward attosecond time-resolved imaging of electron motion in atoms and molecules [20]. In this study, we focus on time-independent scenarios. Fig.2 depicts triangular and parabolic potential barriers.

For a one-dimensional particle passing through a potential barrier of arbitrary shape between lengths $|a, b|$, the probability can be expressed using the Eq.(13)

$$D = D_0 exp\left(-\frac{2}{\hbar}\int_a^b \sqrt{2m(U(x)-E)}dx\right). \tag{13}$$

By ignoring changes in the quantity $D_0$ concerning the exponent and setting it to 1, the transmission coefficient of a particle with energy $E$ through the potential barrier shown in Fig.2(a) can be determined. This involves substituting the potential energy from $U(x) = E + \frac{U_0}{l}x$ into Eq.(13) and integrating between points F and C. The analytical calculations and the resulting expression are provided in Eq.(14):

$$-\frac{2}{\hbar}\int_{x_1}^{x_2}\sqrt{2m(U(x)-E)}dx = -\frac{2}{\hbar}\int_{x_1}^{x_2}\sqrt{2m\left(E+\frac{U_0}{l}x-E\right)}dx = -\frac{2}{\hbar}\sqrt{2m}\cdot\int_{x_1}^{x_2}\sqrt{\frac{U_0}{l}x}dx =$$
$$-\frac{2}{\hbar}\sqrt{2m}\cdot\sqrt{\frac{U_0}{l}}\cdot\int_{x_1}^{x_2}\sqrt{x}dx = -\frac{2}{\hbar}\sqrt{2m\frac{U_0}{l}}\cdot\frac{x^{\frac{3}{2}}}{\frac{3}{2}}\Big|_{x_1}^{x_2} = -\frac{4}{3\hbar}\sqrt{2m\frac{U_0}{l}}\cdot\left(x_2^{\frac{3}{2}}-x_1^{\frac{3}{2}}\right) = -\frac{4}{3\hbar}\sqrt{2m\frac{U_0}{l}}\cdot$$
$$\left(\left(l-\frac{E}{U_0}l\right)^{\frac{3}{2}}-0^{\frac{3}{2}}\right) = -\frac{4}{3\hbar}\sqrt{2m\frac{U_0}{l}}\cdot l\sqrt{l}\cdot\frac{1}{U_0\sqrt{U_0}}(U_0-E)^{\frac{3}{2}} = -\frac{4}{3\hbar}\sqrt{2m}\cdot\frac{l}{U_0}(U_0-E)^{\frac{3}{2}}$$
$$D = exp\left(-\frac{4\sqrt{2m}}{3\hbar}\cdot\frac{l}{U_0}(U_0-E)^{\frac{3}{2}}\right) \tag{14}$$

To determine the transmission coefficient of a particle with energy E through the potential barrier shown in Fig.2(b), we need to substitute the potential energy function $U(x) = U_0\left(1-\frac{x^2}{l^2}\right)$

into Eq.(13) and integrate between the coordinates $x_1$ and $x_2$. The analytical calculations and the resulting expression are provided in Eq.(15):

$$-\frac{2}{\hbar}\int_{x_1}^{x_2}\sqrt{2m\left(U_0\left(1-\frac{x^2}{l^2}\right)-E\right)}\,dx=-\frac{2\sqrt{2m}}{\hbar}\int_{x_1}^{x_2}\sqrt{U_0-U_0\frac{x^2}{l^2}-E}\cdot dx=$$
$$-\frac{2\sqrt{2m}}{\hbar l}\int_{x_1}^{x_2}\sqrt{U_0l^2-U_0x^2-El^2}\cdot dx=-\frac{2\sqrt{2m}}{\hbar l}\int_{x_1}^{x_2}\sqrt{(U_0-E)l^2-U_0x^2}\cdot dx=$$
$$-\frac{2\sqrt{2mU_0}}{\hbar l}\int_{x_1}^{x_2}\sqrt{\left(1-\frac{E}{U_0}\right)l^2-x^2}\cdot dx.$$

Perform the following assignment: $\left(1-\frac{E}{U_0}\right)l^2\equiv a^2;\ a^2=x_{1,2}^2$,

$$-\frac{2\sqrt{2mU_0}}{\hbar l}\int_{x_1}^{x_2}\sqrt{a^2-x^2}\cdot dx=-\frac{2\sqrt{2mU_0}}{\hbar l}\left(\frac{x\sqrt{a^2-x^2}}{2}+\frac{a^2}{2}arcsin\frac{x}{a}\right)\Big|_{x1}^{x_2}=-\frac{2\sqrt{2mU_0}}{\hbar l}\Big[0+$$
$$\frac{a^2}{2}arcsin\frac{x_2}{a}-\left(0+\frac{a^2}{2}arcsin\frac{x_1}{a}\right)\Big]=-\frac{2\sqrt{2mU_0}}{\hbar l}\left[\frac{a^2}{2}\arcsin(1)-\frac{a^2}{2}\arcsin(-1)\right]=-\frac{2\sqrt{2mU_0}}{\hbar l}\frac{a^2}{2}2\cdot$$
$$\arcsin(1)=-\frac{2a^2\sqrt{2mU_0}}{\hbar l}\cdot\frac{\pi}{2}=-\frac{a^2\sqrt{2mU_0}}{\hbar l}\cdot\pi=-l^2\left(1-\frac{E}{U_0}\right)\frac{\sqrt{2mU_0}}{\hbar l}\cdot\pi=-\frac{\pi l}{\hbar}(U_0-E)\cdot\sqrt{\frac{2m}{U_0}};$$
$$D=\exp\left(-\frac{\pi l}{\hbar}\cdot\sqrt{\frac{2m}{U_0}}(U_0-E)\right). \qquad (15)$$

## 5. Problem 2: Results and discussion

Using the *Numpy* and *Matplotlib* libraries in the Python programming environment, a program was created to plot the tunneling coefficients of particles as a function of energy $E$ in two scenarios. The graphs were generated using 100 data points. The following designations were used in the calculation program: $m_ec^2=0.511\,MeV$, $l=2A^0$, $\hbar c=197\,MeV\cdot fm, 1fm=10^{-15}m$, considering the electron as the particle. The discussed quantities are presented in units of $eV$ and $m$. Fig.3 shows the tunneling coefficients of a particle with triangular and parabolic potential barriers as a function of the particle's energy. It is noted that the tunneling coefficient for a triangular-shaped barrier is greater than that for a parabolic-shaped barrier at the same energy value.

Fig.4(a) shows the tunneling coefficients of a particle with triangular and parabolic potential barriers as a function of the barrier width. The figure shows that the tunneling coefficient is smaller for the same barrier width when the barrier is triangular. Specifically, for $x_0=0.5\cdot10^{-10}m$, is $D(x_0)=0.1$ for the triangular barrier (blue curve) and approximately $D(x_0)\approx0.3$ for the parabolic barrier (red curve). Additionally, the tunneling coefficient quickly approaches 0 if the barrier width exceeds two angstroms ($x>2\cdot10^{-10}m$). Fig.4(b) shows the tunneling coefficients of a particle with triangular and parabolic potential barriers as a function of the barrier width when the particle mass is 2000 times greater than the rest mass of the electron: $m_{nuclon}\approx2000m_e$. At the same barrier height, the tunneling coefficient decreases significantly for widths $x>4pm$.

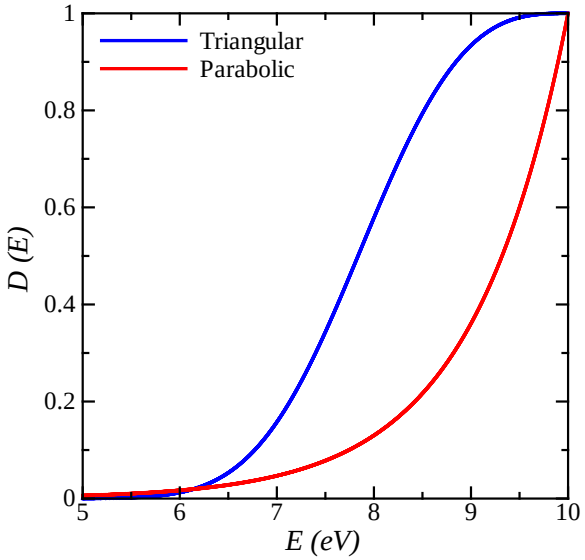


**Fig. 3**. Dependence of the tunneling coefficient $D$ on the energy $E$ of a particle passing through triangular-shaped (blue curve) and parabolic-shaped (red curve) potential barriers.

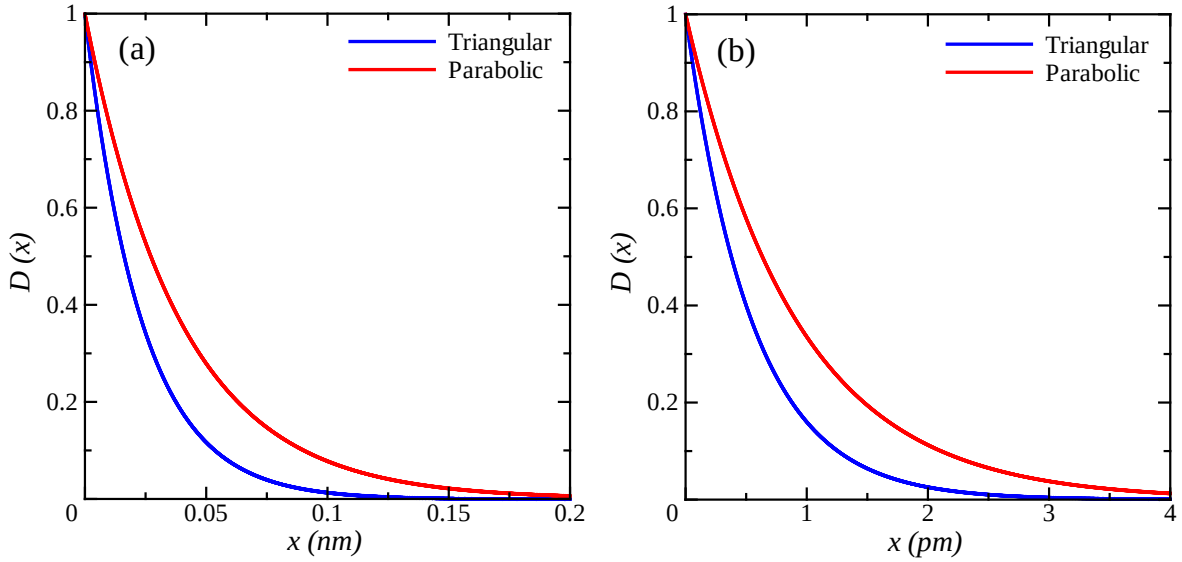


**Fig. 4**. Dependence of the tunneling coefficient $D$ on the width of the barrier $x$ for (a) particle and (b) nucleon passing through triangular-shaped (blue curves) and parabolic-shaped (red curves) potential barriers.

## 6. Conclusions

The paper explores stationary problems of the Schrödinger equation. The initial focus is deriving the probability distribution of electrons in the hydrogen atom within a spherical system, determined by recursive coefficients. Using Python, probability distribution curves for electrons in hydrogen atoms and helium ions were plotted based on distance. The analysis reveals that the probability of electron distribution at a given excited level decreases as the atomic number $Z$ increases. This occurs because the coefficients governing the wave function decrease with the increasing magnitude of $\sigma$, which, as per Eq.(2), varies directly with $Z$.

The second part of the study addresses the transmission of a quantum particle with specific energy through two types of potential barriers: triangular and parabolic. Utilizing a Python program, tunneling coefficients were computed under varying particle energies and distances. The results indicate that the tunneling coefficient is smaller for the same barrier length when the barrier is

triangular. It was further shown that the tunneling coefficient is higher for a given particle energy when the barrier is triangular. Similar analyses were conducted for nucleons ($m_{nuclon} \approx 2000m_e$), revealing that the tunneling coefficient decreases as the barrier width exceeds $x > 4pm$ at a constant barrier height.

## Acknowledgments

This work was supported by the Scientific Research Grants through the Higher Education and Science Committee of Ministry of Education, Science, Culture and Sports of Armenia (21AG-1C061).

**References**

[1]. P. Mohile, A. Ahmed, T.R. Vishnu, P. Ramadevi, arXiv:2309.00026, 2023.
[2]. M.Gh. Al-Masaeed, E.M. Rabei, A. Al-Jamel, Progress in Fractional Differentiation and Applications **10** (2022) 137.
[3]. L.D. Landau, E.M. Lifshitz, Quantum Mechanics, Non-Relativistic Theory (Pergamon Press, Oxford, 1977).
[4]. D. Bohm, Quantum Theory (Dover Publications, New York, 1989).
[5]. W.P. Schleich, D.M. Greenberger, D.H. Kobe, M.O. Scully, PNAS **110** (2013) 5374.
[6]. C.D. Richardson, P. Schlagheck, J. Martin, N. Vandewalle, Th. Bastin, Phys. Rev. A **89** (2014) 032118.
[7]. Y. Oba, N. Watanabe, T. Hama, K. Kuwahata, H. Hidaka, A. Kouchi, The Astrophysical Journal **749** (2012) 67.
[8]. S. Spicklemire, Visualizing Quantum Mechanics with Python (CRC Press, 2024).
[9]. V.V. Skobelev, Rus. Phys. J. **64** (2021) 1328.
[10]. L.G. Mardoyan, G.S. Pogosyan, A.N. Sisakyan, V.M. Ter-Antonyan, Theor. Math. Phys. **61** (1984) 1021.
[11]. Y. Tomiie, J. Phys. Soc. Jpn. **13** (1958) 1030.
[12]. R.B. Coats, D.R. Howe, Int. J. Math. Edu. Sci. Technol. **5** (1974) 685.
[13]. J.J. Sakurai, J. Napolitano, Modern Quantum Mechanics (Cambridge University Press, 2020).
[14]. Repository: Quantum Mechanics Python Solutions, available at https://github.com/hasmikshahinyan/quantum-mechanics-python-solutions-2024.
[15]. B.R. Holstein, Am. J. Phys. **64** (1996) 1061.
[16]. S. Coleman, Phys. Rev. D. **15** (1977) 2929.
[17]. B.D. Josephson, Phys. Lett. **1** (1962) 251.
[18]. K. Shukla, P.S. Chen, J.R. Chen, Y.H. Chang, Y.W. Liu, Commun. Phys. **3** (2020) 101.
[19]. G. Lazarides, R. Maji, Q. Shafi, J. Cosmol. Astroparticl. Phys. **5** (2024) 128.
[20]. M. Yu, K. Liu, J. Yan, Ch. Cao, J. Tan, J. Liang, K. Guo, W. Cao, P. Lan, Q. Zhang, Y. Zhou, P Lu, Light Sci. Appl. **11** (2022) 215.